Progress Toward a CdTe Cell Life Prediction

T.J. McMahon and G.J. Jorgensen

National Renewable Energy Laboratory, Golden, CO. 80401

Abstract. In this paper, we review the progress made by the CdTe Thin Film Partnership Reliability Team in developing an accelerated environmental test (AET) methodology that will indicate the expected life of CdTe cells incorporated in a module operated in the field. The primary focus is on test design, cell reliability, and the correlation of indoor accelerated testing with outdoor exposure. The team has emphasized cell-stability issues, and is not examining failure modes such as those involving module packaging, junction boxes, and mounting. The goal is to develop a CdTe cell technology with a 30 yr life, and verify that reliability through AETs.

BACKGROUND

The CdTe Thin Film Partnership Team is composed of five industrial members {British Petroleum [BP], Canrom, Golden Photon, Inc. [GPI], ITN Energy Systems, and Solar Cells, Inc. [SCI]}, four universities {Colorado State University [CSU], Colorado School of Mines [CSM], University of South Florida [USF], and University of Toledo [UT]}, three Laboratories {Florida Solar Energy Center [FSEC], Institute of Energy Conversion [IEC], and National Renewable Energy Laboratory [NREL]} and one consultant, Alan Fahrenbruch [ALF]. Two years ago, the team expressed a desire to develop a stability-testing protocol for CdTe modules with the intent of predicting module life. This is an aggressive goal requiring extensive cross-cutting expertise, including analytical characterization, statistical analysis, and material science. We have chosen to examine those failures related to CdTe cell and interconnect technology rather than the entire module for two reasons: 1) the expertise available on this team is more suited to cell issues, and 2) the first-order question is whether or not the thin film CdTe cells can be made to withstand the hazards of outdoor exposure. The preliminary accelerated-life-test protocol calls for 11 combinations of cell bias, light level, and temperature plus UV and interconnect tests.

Accelerated environmental tests (AETs) are being used in two ways. The first is in standardized screening tests. Screening tests require a small number of test samples to accelerate and isolate failure modes and can be performed on minimodules or cell structures. The basic approach here is to prioritize failure modes to be investigated, design and perform AETs to fully characterize each individual failure mode (in terms of relevant environmental stresses), and repeat the process with each succeeding failure mode until all are understood. In this way, these screening tests will reveal relevant failure mechanisms and allow acceleration factors to be determined for the different models that are used in the second type of AET, namely, life-prediction tests.

The second way of using AETs is in life-prediction testing. Lifetime-prediction tests appropriate for the complete CdTe module will require a large number of test samples, and will follow at an appropriate time when a final module design is defined, all failure

CP462, *NCPV Photovoltaics Program Review*,
edited by M. Al-Jassim, J. P. Thornton, and J. M. Gee
1999 The American Institute of Physics 1-56396-836-3/99/$15.00

modes are identified, and acceleration parameters for each relevant environmental stress are known. The AETs chosen must use stress or combinations of stresses that will accelerate those failure modes likely to occur in the real world. Refs. 1 - 3 provide excellent summaries of the methodologies that are generally applicable to a wide variety of materials and devices, including PV cells and modules.

Life-prediction testing can be divided into five steps: 1) identify and isolate all of the failure modes; 2) design and perform AET; 3) use appropriate distributions to model specific failure rates; 4) choose and apply relevant acceleration models to transform failure rates; 5) develop a total module failure rate as a composite of individual rates to allow prediction of life in a field environment. These steps are explained below.

Based on their experience with such devices, members of the CdTe Stability Team have identified a number of known and suspected failure modes; these are listed in Table 1, along with possible failure mechanisms that could lead to these failure modes. It is important to understand the dominant forms of degradation to allow transformation from life at accelerated stress to life at use-stress conditions, and to allow problems to be remedied and improvements in reliability to be made.

TABLE 1. CdTe Failure Modes and Failure Mechanisms

Failure Modes	**Possible Failure Mechanisms**
Cell Degradation	
a. Main junction: increased recombination	Diffusion of dopants, impurities, etc. Electromigration
b. Back barrier; loss of ohmic contact	Diffusion of dopants, impurities, etc. Corrosion, oxidation Electromigration (field-induced diffusion?)
c. Shunting	Diffusion of metals, impurities, etc.
Interconnect Degradation	
a. Interconnect resistance	Corrosion Electromigration
b. Shunting	Corrosion Electromigration
Busbar Degradation	Corrosion Electromigration
Encapsulation Failure	
a. Delamination	Surface contamination
b. Loss of hermetic seal	Bulk degradation
c. Loss of high-potential isolation	Photodegradation

The key to the use of accelerated testing for life-prediction purposes is the relation of time at use stress (t_u) to time at elevated/accelerated stress (t_s) via a linear acceleration factor (a_i)(4):

$$t_u = a_i t_s \quad , \tag{1}$$

where the failure mechanism for accelerated conditions is assured to be the same as that experienced during field conditions. The type of failure mode experienced relates relevant stress factors to a_i. For example, diffusion and oxide-formation failure mechanisms are thermally driven, and an Arrhenius treatment may be appropriate. In such a case, the form of the acceleration function can be used to relate the time-dependent loss in performance (degradation), $\Delta P(t)$, at a particular elevated temperature, T_S as:

$$\Delta P(t) = Ae^{-E/T_S}\Delta t \quad . \tag{2}$$

The life at this stressed condition, t_S, is the time, Δt, at which performance degrades below some level that defines failure. $\Delta P(t)$ is measured at intervals of AET exposure to an elevated, laboratory-controlled temperature T_S. The activation energy, E, is obtained by fitting the data to Equation (2) for at least three values of T_S, with one near or at T_U. Once E is known, the Arrhenius acceleration factor can be used in Equation (1) to obtain time to failure (lifetime) at a given use temperature, T_U, as:

$$t_u = e^{-E\left[\frac{1}{T_S} - \frac{1}{T_U}\right]} t_s \quad . \tag{3}$$

Of course, in real world operation, a single constant use-temperature is not realistic. To project field life at a "typical" location characterized by a given yearly temperature distribution such as shown in Figure 1, the time, t_{uj} at each use-temperature

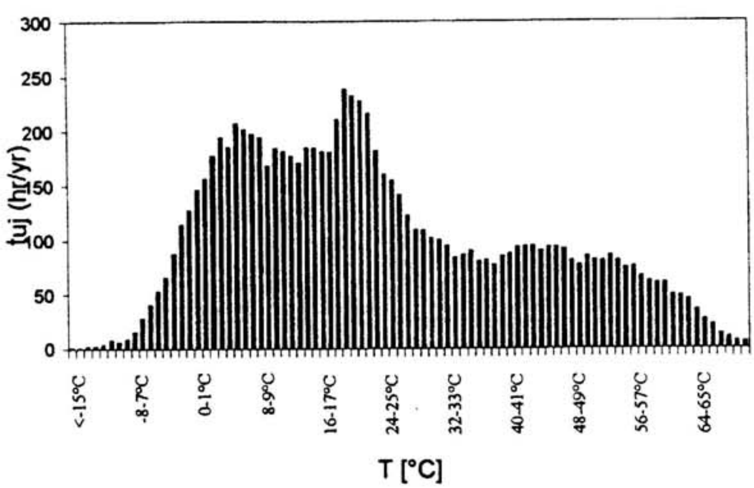

FIGURE 1. Back-of-Module Temperatures for Las Cruces, NM

experienced, T_{uj}, can be computed, and the overall lifetime would then be:

$$t_u = \frac{1}{\sum_j \frac{\gamma_j}{t_{uj}}} = \frac{t_s}{\sum_j \gamma_j e^{E\left[\frac{1}{T_S} - \frac{1}{T_{uj}}\right]}} \tag{4}$$

where γ_j is the number of hours per year that the module experiences T_{uj}. The results of Equation (4) are plotted in Figure 2 where the time at a constant stress temperature required to simulate 1 year's exposure at three different sites is shown for three activation energies. Note that for E = 0 eV there is no temperature dependence and all three sites degenerate into one horizontal line at t_S = 8670 h. We will use the results this graph later.

For life-prediction purposes, PV modules can be modeled as a series system (4) in which the device has a potential time-to-failure for each of M competing failure modes. The life of such a system is the smallest of those M potential times to failure, and the system fails when the first failure mode occurs. If the different times-to-failure associated with the M modes are statistically independent, then the failure-rate function, h(t), follows the addition model for failure rates:

$$h(t) = \sum_{i=1}^{M} h_i(t) \tag{5}$$

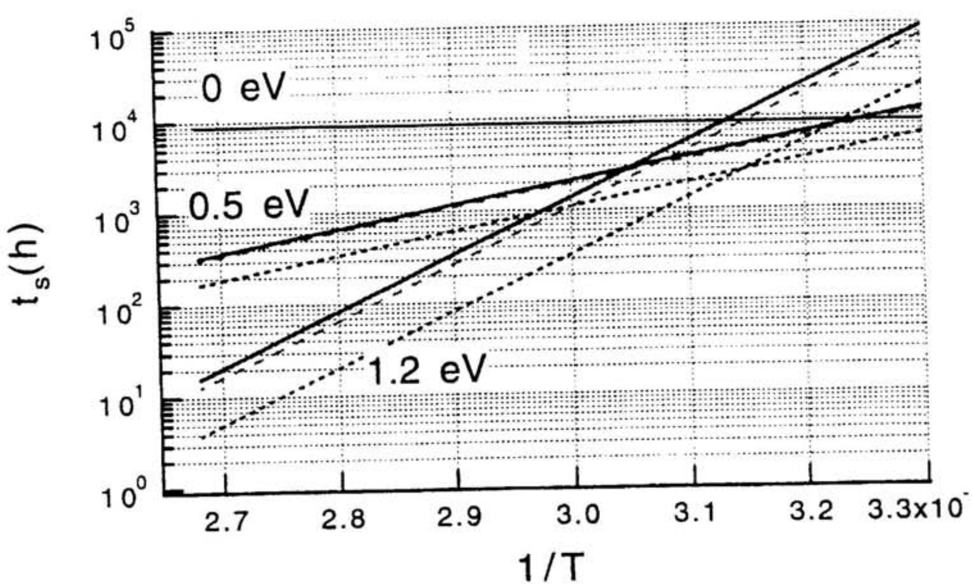

FIGURE 2. Stress time, t_S, to simulate 1 year at Superior, CA (solid lines), SWDTI (dashed lines) and NREL (dotted lines), for E = 0 eV, 0.5 eV, and 1.2eV.

or, for a PV module:

$$h_{module}(t) = \sum_{i=\text{cell, bus, contact, etc.}} \left[h_{elec}(t) + h_{diff}(t) + h_{corr}(t) + \ldots\right]_i \quad . \qquad (6)$$

Once the failure rate is known, the expected life or mean time to failure (MTTF) can be calculated as:

$$MTTF = \int_0^{\infty} t \cdot h(t) \cdot \exp\left[-\int_0^t h(t)\,dt\right] dt \quad . \qquad (7)$$

Isolating Failure Modes Through AETs

T team has worked on designing AETs to isolate cell failure modes and identifing the responsible failure mechanisms (steps 1 and 2 above). Stress tests are applied to cell structures made by various fabrication processes, principally variation in the back-contact recipe. These screening tests require only a small number of test samples. For characterization, we measure J_{SC}, V_{OC}, FF, and R_{OC} from the light I-V curves at various time intervals during stress testing. R_{OC} is the slope of the light I-V curve at V_{OC}. Change in series barrier effects, measured from dark I-V data at different temperatures, is also used to monitor degradation during the accelerated testing.

Three types of change in cell I-Vs have been noticed as a result of stress testing, which may be caused by different failure mechanisms: 1) an increase in R_{OC} and "rollover" in the I-V at voltages larger than V_{OC}, possibly from back contact barrier formation, 2) a reduction in V_{OC}, and 3) an increase in the slope of the I-V curve through J_{SC}, possibly from increased shunting (5, 6) or from increased recombination in the space-charge region. The thermal acceleration being measured for the loss in peak power efficiency during these screening tests at 100°, 85°, and 65° C has yielded an activation energy as high as 1.2 eV on cells with one of the back contacts(7). Temperature-dependent I-V curves yield a barrier height of 0.3 eV.(8) Another feature of this failure mechanism is that cells and modules are found to be much less stable when stressed at V_{OC} rather than either P_{max} or J_{SC}(6,7). CSU finds a loss of $\Delta P(t)$ = 10% may take 50 times longer to occur at P_{max} than at V_{OC} for some cells.

To further separate the increase in R_{OC} from an increase in series resistance, we conducted accelerated tests on two CdTe cells with different back-contact recipes. After 60 hr at 90° C, we find a small change in one cell's light I-V, but the dark I-V is rolling over badly. On the other cell, we find rollover with degradation in both the light and dark I-Vs. Internal cell resistance measurements (9) on these two cells before and after stress at 90° C for 60 hr show that the internal series resistance is increased by approximately 40%, but since the starting values are only a few 10^{-3} ohm cm^2, it is really the formation of back contact barrier that is contributing to the high values of R_{OC} and rollover, and not series resistance.

Identifying Failure Mechanisms

To understand the failure mechanism causing the non-ohmic back junction, two ideas have been suggested by team members: a loss in acceptor density in the p^+ layer is one, and an oxide interface layer (10) is the other. This team is stressing cells made with many different back-contact recipes, including cells without back contacts to search for the source of the rollover with its subsequent losses in FF and V_{OC}. Various back contacts were made on common CdTe substrates finished through the $CdCl_2$ treatment. Initial screening studies show degradation times vary from days to weeks at 100° C depending on the back contact recipe (CSU).

Back-contact recipes vary greatly, but almost without exception use Cu as the p-type dopant. Cu is introduced as a thin metal film (IEC, CSM), as a Cu salt in a graphite suspension (USF, NREL), or in a doped ZnTe contact layer (NREL). Degradation caused by loss-in-acceptor density in the p^+ layer suggest models using global diffusion of impurities or local defect conversion to explain the degradation of the cell I-V characteristic(CSM). Capacitance-voltage profiling (CSM, CSU) and photoluminescence studies (NREL) are additional nondestructive methods applied to cells before and after AETs to determine the failure modes. For diffusion failure models, Cu with a diffusion coefficient of $5x10^{-14}$ cm^2/sec at 100° C and activation energy of 0.66 eV(11) is a prime suspect. A back-of-the-envelope calculation indicates that a diffusion coefficient of $3x10^{-14}$ cm^2/sec is required to move or change the charge state of enough acceptors in the back contact region to cause contact failure within 1 hour. Remembering that cell degradation can depend on bias, we note that even in diffusion processes, the charge state of vacancies can affect the rate of a diffusing atom. The team is including effects due to the three-dimensional nature of CdS/CdTe grains and grain boundaries and the effect on diffusion, electromigration of charged atoms, and local compensation effects in degradation models.

The importance of the oxide layer between the p-CdTe and the metal/carbon contact is being revisited. The growth of an interphase oxide along with possible change in the acceptor concentration in the CdTe at the interface could account for some previously unexplained observations on stressed cells. For example, 1) the activation energy for oxide growth is 1.2 eV (12), more in line with the higher T-dependences found by CSU (i.e. 1.2 eV); 2) a study on stressed, uncontacted cells finished through the Cu diffusion, showed a shift in Voc, but no rollover, after contacting (IEC) (see Ref. 10 for I-V curves for oxide barrier devices); 3) I-V characteristics for far forward bias in cells exhibiting rollover which do not breakdown for as much as a volt; and 4) a bluish film is usually found when the back-metal contact is removed. These observations are better explained with a back-surface insulating interface model. Studies involving back-contact removal experiments principly at IEC and now at NREL are starting to produce results.

Another effort to locate the source of degradation involves recontacting degraded cells in an attempt to resurrect the cell properties. The results have been mixed: IEC finds that recontacting removes the rollover, but the V_{OC}-shift remains, while USF finds that 25% of the loss in V_{oc} and 71% of the fillfactor is restored. AMPS device modeling (ALF) and discrete device modeling (IEC) are applied to temperature-dependent I-V data to explain cell performance and define a parameter to quantify failure modes. Initially, one-dimensional models will be used. Two- and three-dimensional AMPS models will be applied eventially to accommodate the grain and grain-boundary properties of the CdTe cell. Global diffusion, electro-migration, local compensation, and oxide-formation failure mechanisms are in need of far more study. Failure mechanisms such as these must be understood before we develop accelerated tests capable of predicting module life with any certainty.

Cell Life Prediction

We now show estimates for two cell-life predictions based on hypothetical numbers not too unlike cell stress data. Yearly temperature histograms for five sites that have CdTe back-of-module temperatures monitored at least hourly have been analysed. Figure 1 shows temperature data gathered at Southwest Technology Development Inst. (SWDTI) in Las Cruces, NM. It is one of the hottest sites. Calculation of an expected life is always subject to a specific use condition, site environment, and the definition of failure. To avoid te issue of defining failure we generally establish life at the times for which a 10% and 25% loss in P(t) occurs. Cell stress degradation data have shown stability to 10% out to 50,000 h at 100° C with E = 0.5 eV under one sun operating at P_{max}. Assuming a linear dP/dt, this yields an expected life of 156 years at SWDTI. Another less stable recipe showing stability to only 600 h at 65° C (with E = 1.2 eV under one sun at V_{oc}) will have a predicted life of 3.3 years at NREL. We see that a predicted life depends on cell fabrication, operating point, and site environment.

Correlation with Field Experience

We need evidence for correlation between degradation of cells in field-exposed CdTe modules and the AET results on CdTe cells. As stated, we do not want to force failures with AETs that will not occur in the field. The problem is that: 1) the cumulative higher-temperature exposure of fielded modules has not been long enough, and 2) baseline data taken on field-exposed modules has not been of the type that would reveal early onset of failure or be able to distinguish between failure modes.

At NREL, we have good documentation on dozens of CdTe modules left outside for 4 years; three were left at V_{oc}, the condition under which we expect the fastest change. Of those, two changed by less than 1% and one increased by 6%. In the 1996 back-of-module temperature histogram from NREL we find lower temperatures topping out at 65° C. Hundreds of hours of exposure at T=65° C are needed to determine any trend. CdTe cell and module-performance data generally show an initial increase before degradation sets in. The remaining modules outdoors at NREL are at P_{max}, a condition that shows degradation as much as 50 times slower. So at P_{max} we are even further away from gathering decisive real-time reliability data.

Another source of field-exposure data for hot temperatures is the two 25-kW CdTe arrays at Edwards Air Force Base in California. Baseline module data are available from the manufacturer. Temperature histogram from a nearby Si system at Superior Valley shows more hours at the hotter back-of-module temperatures than at SWTDI. Real-time reliability data will become available to correlate with our AETs.

CONCLUSIONS

Preliminary cell life predictions for two hypothetical sets of data were presented to demonstrate the methodology. The rate of loss in performance depends on the back contact applied to the cell, the operating bias, and the use temperature. Results from the AETs currently being used must be correlated with outdoor field exposure. A functional dependence on time of P(t) needs to be established. This team is working hard to reveal the failure mechanisms causing the losses in performance during AETs.

ACKNOWLEDGEMENTS

We wish to thank D. King, G. Rich, C. Whittaker, and B. Kroposki for the site-temperature histogram data. This work is supported under DE -AC36-83CH10093.

REFERENCES

1. J. W. Martin, S. C. Saunders, F. L. Floyd, and J. P. Wineburg, "Methodologies for Predicting the Service Lives of Coating Systems," National Institute of Standards and Technology Building Science Series 172, Gaithersburg, MD, October 1994.
2. A. Czanderna, G. Jorgensen, "Service Lifetime Prediction for Encapsulated Photovoltaic Cells/Minimodules," *AIP Conf. Proc. 394, 14th NREL/SNL Photovoltaics Program Review*, C. E. Witt, M. Al-Jassim, and J. M. Gee, eds., American Institute of Physics, Woodbury, NY, 1997, pp. 295-311.
3. William Q. Meeker, Gerald J. Hahn, "How to Plan an Accelerated Life Test - Some Practical Guidlines," *T ASQC Basic References in Quality Control: Stastical Techniques*, J.A. Cornell and S.S. Shapiro, Editors.
4. Nelson, W., *Accelerated Life Testing*, John Wiley and Sons, Inc., New York, 1990.
5. P. V. Meyers, M. M. Al-Jassim, and S. Asher, "A Search for Degradation Mechanisms of CdTe/CdS Solar Cells," Proceedings of the Materials Research Society, April 11, 1996, San Francisco, CA.
6. R.C. Powell, R. Sasala, G. Rich, M. Steele, K.Bihn, N. Reiter, S. Cox and G. Dorer, "Stability Testing of CdTe/CdS Thin-Film Photovoltaic Modules," 25th IEEE PV Spec. Conf., Washington, DC, p.785 May 1996.
7. Jason Hiltner and James Sites, private communication.
8. G. Stollwerck, J.R. Sites, "Analysis of CdTe Back Contact Barriers," European conference, p. 2020.
9. A.E. Delahoy and Adam M. Payne, "Determination of the Internal Series Resistance of CIS and CIGS Photovolaic Cell Structures," 25th IEEE PV Spec. Conf., Washington, DC, May 1996.
10. V.P. Singh, O.M. Erickson, and J.H. Chao, J. Appl. Phys. 78(7) p.4538 (1995).
11. H.H. Woodbury and M. Aven, J. Appl. Phys. 39(12) p.5485 (1968).
12. F. Wang, A. Schwartzman, A.L. Fahrenbruch, R. Sinclair and R.H. Bube, J. Appl. Phys. 62(4) p.1469 (1987).